

复用加权二进制编码条纹三维测量方法

严飞^{1,2}, 路长秋¹, 文杰¹, 肖雨倩¹, 刘佳^{1,2*}¹南京信息工程大学自动化学院, 江苏 南京 210044;²江苏省大气环境与装备技术协同创新中心, 江苏 南京 210044

摘要 二值条纹不受三维测量系统非线性伽马效应的影响,同时能显著提高投影效率。基于此,提出一种复用加权二进制编码条纹方法以实现三维测量。首先,对传统正弦条纹的灰度进行特定均匀采样,使用二进制编码条纹方法生成8幅二值条纹。然后,对二值条纹组合进行唯一化处理,将4幅相异的二值条纹投影到被测物体表面,对采集到带有物体表面调制信息的二值条纹进行复用二进制加权运算,生成调制后的正弦条纹。最后,对该方法开展了多组对照实验。实验结果表明,所提方法将用于加权生成正弦条纹的二值条纹优化为4幅后,仍然可以保持良好的测量精度和效果。所得标准球的局部点云与拟合标准球的平均距离,相比于传统三步相移技术降低了72.3%。

关键词 三维测量; 相移技术; 二进制编码; 二值条纹; 非线性

中图分类号 TN247

文献标志码 A

DOI: 10.3788/AOS222116

1 引言

结构光投影技术因其非接触、高精度、低成本等优点,成为光学三维测量的重要研究方向之一,已广泛应用于生物识别、逆向工程、工业制造以及机器视觉等多重领域^[1-3]。在众多结构光三维测量技术中,条纹投影轮廓术^[4-7],又称为光栅投影轮廓术被广泛应用,包括相位测量轮廓术(PMP)与傅里叶变换轮廓术(FTP)。通过投影多幅不同相位差的正弦条纹图像到被测物体表面,PMP技术可以独立地获取每个像素点的相位信息,测量精度高^[8-10]。

PMP技术中的误差主要有两个来源:相移误差和系统的非线性误差。与传统的光栅投影相比,基于数字光投影的测量优点是利用计算机产生标准的正弦条纹,可以消除相移误差,可将任意形状和周期的标准正弦条纹通过数字投影仪投射到被测物体^[11]。为了降低系统的非线性误差的影响,国内外学者的提出了多种解决方案,本研究将其概述为3大类。1)误差补偿法。误差补偿法根据标定出的系统误差分布规律,对带有物体调制信息的变形条纹进行补偿,例如Zhang等^[12]事先标定出系统的非线性误差表,使用查找表的方法对变形条纹在 $(-\pi, \pi]$ 的截断相位进行补偿,可以大大降低投影仪非线性引起的相位误差,此类方法对环境光强的稳定性要求较高,在系统环境变化时需要重新标定。反向误差补偿法通过额外投影相移条纹图像

降低非线性误差,例如郑东亮等^[13]使用双四步、双五步相移法有效减小了非线性误差,但双步相移法需要多投影一倍的相移条纹。2)离焦投影法。SU等^[14]使用二值条纹离焦投影的测量方法,在降低投影仪非线性影响的同时显著提高了数字投影仪的投影速率,但该方法难以控制离焦量,且会因离焦投影降低测量的景深范围。3)二值条纹叠加法。该方法通过投影多幅二值条纹到被测物体表面,再通过特殊叠加的方式生成带有物体调制信息的正弦条纹图像。严飞等^[15]提出二值编码条纹聚焦投影的方法,将二值条纹编码成为单个周期内对称、两端白色条纹逐渐向中间位移的多幅编码图案,通过正弦系数叠加生成正弦条纹。刘佳等^[16]提出二进制编码条纹的方法,先对正弦条纹一个周期内的光强值进行二进制编码,再将“0”“1”码字组合成二值条纹,最后通过二进制加权的方式叠加生成正弦条纹图像。此类方法通过投影二值条纹图像代替灰度正弦条纹,实现了二值条纹与相移技术的有效结合,可以降低系统的非线性影响。

本文在二进制编码条纹的基础上,提出复用加权二进制编码条纹方法。在二进制编码条纹的实施过程中,特定的灰度值采样个数下会出现一定的重复二值条纹。经过对比,一个正弦周期内均匀采样12个灰度值,对其十进制进行二进制编码,再将同一位次的“0”“1”码字组合成二值条纹,进行唯一化处理之后,仅需投影4幅相异的二值条纹,通过复用二进制加权运算

收稿日期: 2022-12-08; 修回日期: 2023-01-15; 录用日期: 2023-02-21; 网络首发日期: 2023-03-09

基金项目: 江苏省研究生实践创新计划 (SJCX23_0384)

通信作者: *liuzy@ciomp.ac.cn

即可生成 1 幅正弦条纹。通过对不同灰度值采样个数的二进制编码条纹进行分析,找出多组具有相同二值条纹,并结合不同步数的相移技术,使用互补格雷码方法进行相位展开。实验结果表明,所提方法既保留了二进制编码条纹方法不受系统非线性影响和不会降低测量景深等优点,又可以大幅减少二进制编码条纹方法的投影幅数。同时,由于数字显微镜投影仪投影二值条纹速率远大于灰度正弦条纹^[17],所提方法也进一步提升了二进制编码条纹投影速率。

2 基本原理

2.1 PMP 与互补格雷码

相位测量轮廓术是一种非接触式光学三维测量方法^[18,19]。由计算机生成在一个周期内均匀移动相同相位量的理想正弦条纹图像,通过数字投影仪投影到物体表面,以获取带有深度调制信息的变形条纹,再对其进行解调得到物体的三维形貌。其基本原理是利用多幅相移条纹图像求取截断相位,优势在于可以精确地测定每一个像素的相位值,精度较高且不受物体表面的波动影响。数字投影仪投影的单幅相移条纹图像可以表示为

$$I_n(x, y) = a(x, y) + b(x, y) \cos \left[\varphi(x, y) + \frac{(n-1) \times 2\pi}{N} \right], n = 1, 2, \dots, N, \quad (1)$$

式中: $a(x, y)$ 为背景光强; $b(x, y)$ 为调制度光强; $\varphi(x, y)$ 为相位值; N 为相移步数。截断相位求取原理如下:

$$\varphi(x, y) = -\arctan \left[\frac{\sum_{n=1}^N I_n^c(x, y) \sin(2n\pi/N)}{\sum_{n=1}^N I_n^c(x, y) \cos(2n\pi/N)} \right], \quad (2)$$

式中: $I_n^c(x, y)$ 为 CCD 相机获取到的第 n 幅相移条纹图像。由于是反正切运算,所求相位值被截断在 $(-\pi, \pi]$ 之间,还需对其进行相位展开以恢复成连续的绝对相位。

格雷码辅助相移技术通过投影一组格雷码二值条纹来标记截断相位的级次。 m 幅格雷码图案可以得到 2^m 个级次 k , 对应 2^m 个截断相位区间,利用式(3)将截断相位恢复成绝对相位。但传统的格雷码辅助相位展开方法中,级次边缘和截断相位区间边缘会出现对齐误差,引起跳变问题。而互补格雷码方法^[20]巧妙地解决了这个问题,该方法在格雷码辅助相移技术的基础上,增加投影一幅格雷码图案,在不同的截断相位区间内获取两个错位的级次 k_1 和 k_2 , 利用式(4)进行相位展开,可以有效避免级次边缘和截断相位对齐误差所带来的跳变问题。互补格雷码辅助相位展开过程如图 1 所示。

$$\Phi(x, y) = \varphi(x, y) + 2\pi k(x, y), \quad (3)$$

$$\Phi(x, y) = \begin{cases} \varphi(x, y) + 2\pi k_2(x, y), & \varphi(x, y) \leq -\pi/2 \\ \varphi(x, y) + 2\pi k_1(x, y), & -\pi/2 < \varphi(x, y) < \pi/2 \\ \varphi(x, y) + 2\pi k_2(x, y) - 2\pi, & \varphi(x, y) \geq \pi/2 \end{cases} \quad (4)$$

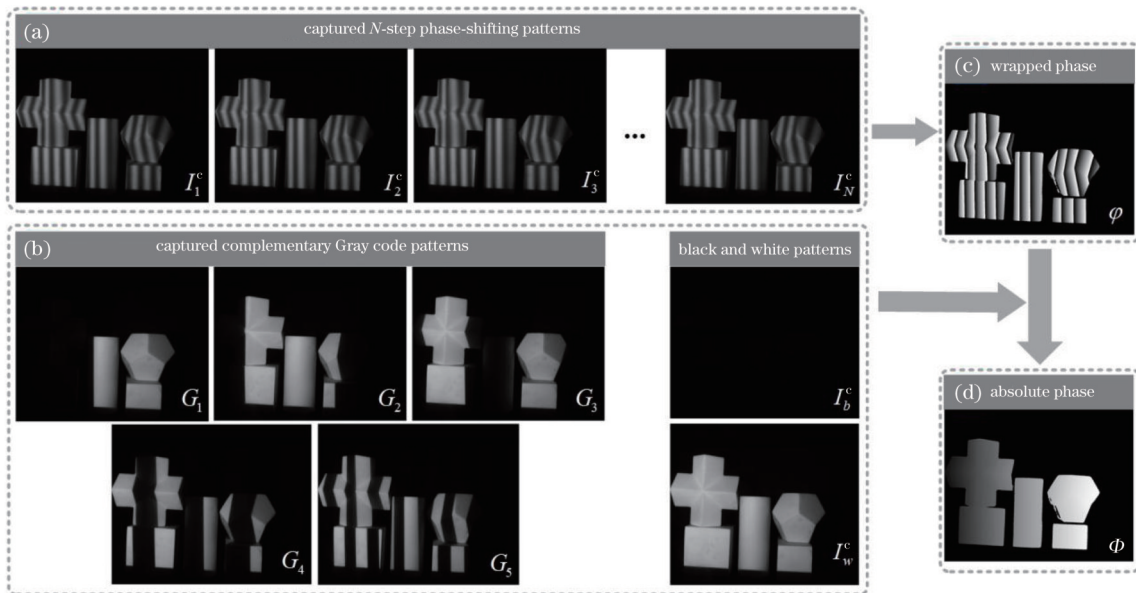


图 1 互补格雷码辅助相位展开。(a) N 步相移图像; (b) 互补格雷码图像; (c) 截断相位图像; (d) 绝对相位图像

Fig. 1 Complementary Gray code assisted phase unwrapping. (a) N -step phase-shifting patterns; (b) complementary Gray code patterns; (c) wrapped phase pattern; (d) absolute phase pattern

2.2 二进制编码条纹原理

二值条纹因只有两个灰度值而不受三维测量系统非线性伽马效应的影响,同时通过数字投影仪投影二值条纹可以大幅提高投影速率。二进制编码条纹方法的提出将二值条纹加权正弦条纹与相移技术有机结合,可以降低系统非线性影响以提高测量精度,同时提高投影速率。

二进制编码条纹从正弦条纹一个周期内灰度值的变化出发,使用均匀采样的方式获取一个周期内若干灰度值,然后对这些十进制灰度值进行二进制转换,再将二进制码的同一位次的“0”或“1”组合成一个周期的二值条纹,并以此扩展到每个周期。正弦条纹的灰度值位于 0 和 255 之间,采样灰度值和二进制转换的过程如下:

$$G_{vm} = 127.5 + 127.5 \times \cos(2m\pi/M), \quad m = 1, 2, \dots, M, \quad (5)$$

$$B_{Gv}^m = \text{Dec2bin}[\text{round}(G_{vm})], \quad (6)$$

式中: G_{vm} 表示采样的第 m 个灰度值; B_{Gv}^m 表示灰度值对应的 8 位二进制码; round 为取整函数; Dec2bin 为十进制数转换成二进制数的函数; M 为采样灰度值个数。每幅二值条纹单个周期内的取值可以表示为

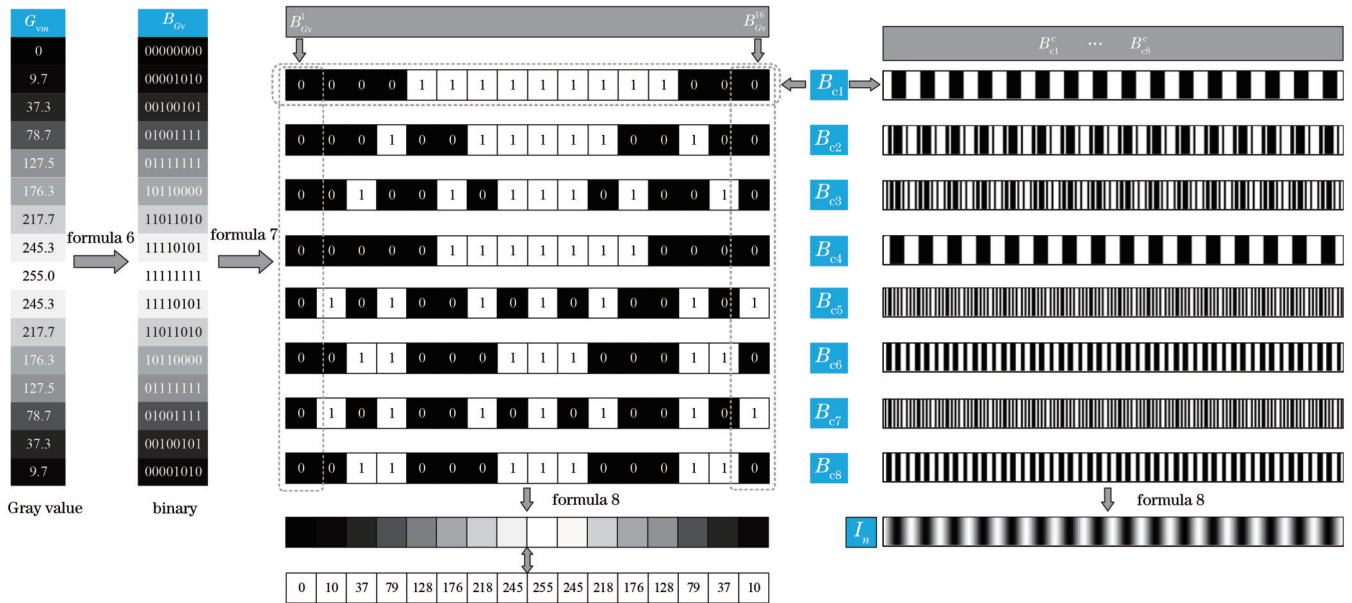


图 2 二进制编码生成二值条纹过程

Fig. 2 The process of generating binary stripes by binary coding

2.3 复用加权二进制编码条纹原理

二进制编码条纹方法^[16]与二值编码条纹聚焦投影方法^[15]从不同的角度实现了二值条纹到正弦条纹的生成。文献^[16]为了提高条纹的正弦性,多投影了 3 幅小数部分的二值条纹,共需要 11 幅二值条纹加权生成正弦条纹。文献^[15]使用 8 幅单个周期内对称且两端白色条纹逐渐向中间位移的多幅二值条纹叠加生成正

$$Z(8, M) = \begin{bmatrix} B_{Gv}^1 \\ B_{Gv}^2 \\ B_{Gv}^3 \\ \vdots \\ B_{Gv}^M \end{bmatrix}^T = [B_{Gv}^1, B_{Gv}^2, B_{Gv}^3, \dots, B_{Gv}^M] = \begin{bmatrix} B_{c1} \\ B_{c2} \\ B_{c3} \\ \vdots \\ B_{c8} \end{bmatrix}, \quad (7)$$

式中: $Z(8, M)$ 为一个 8 行 M 列的矩阵,用于表示二值条纹一个周期内的二值分布; $B_{c1} \sim B_{c8}$ 表示 8 幅二值条纹单个周期内的二值分布。以 m 取 16、条纹周期 T 为 16 为例,对应二值条纹的生成过如图 2 所示。将生成的二值条纹顺序投影到被测物体表面,再用 CCD 相机采集到带有物体深度信息的二值条纹图像,使用式(8)进行二进制加权,可以得到一幅受物体深度调制的正弦条纹图像。

$$I_n^c = \left[\sum_{i=1}^8 (B_{ci}^c - I_b^c) \times 2^{(8-i)} \right] / 255, \quad n = 1, 2, \dots, N, \quad (8)$$

式中: I_n^c 表示叠加生成的第 n 幅相移条纹图像; N 为相移步数; B_{ci}^c 表示为 CCD 相机采集到的第 i 幅二值条纹; I_b^c 为全黑场条纹,此处用于减小所采集二值条纹黑色光强不为 0 的误差,也可以用于第 2.1 节格雷码的二值化处理。图 3 为周期 T 为 8 的二值条纹、加权生成正弦条纹仿真。

弦条纹。

为了减少二进制编码条纹方法投影二值条纹的幅数,提出复用加权二进制编码条纹方法。在二进制编码方法的实现过程中,8 幅二值条纹中会出现重复条纹。例如在 2.2 小节中,当 m 为 16 时,二进制编码方法产生的 8 幅二值条纹中的 B_{c5} 与 B_{c7} 以及 B_{c6} 与 B_{c8} 是完全相同的。因此测量时,对于这些相同条纹仅需投影和

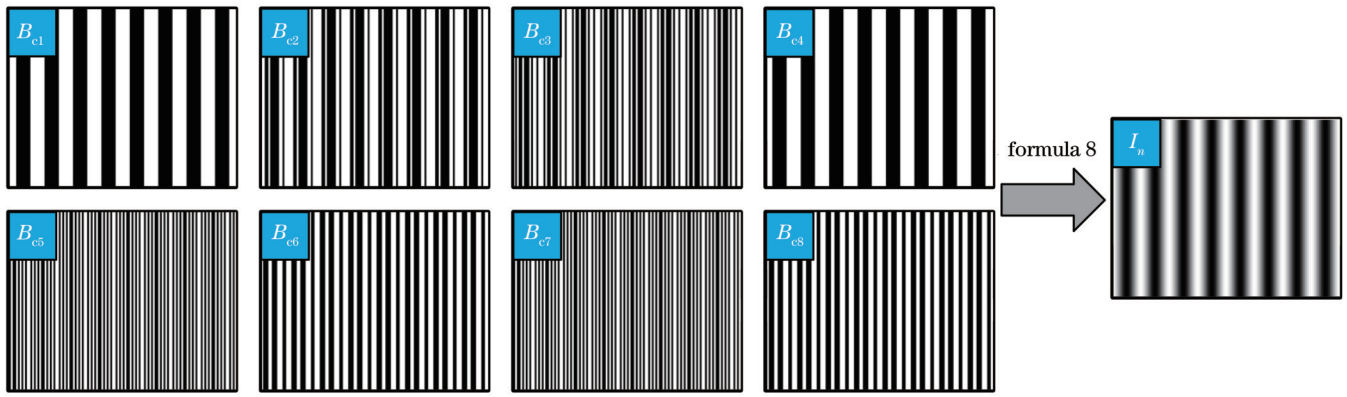


图 3 二值条纹加权正弦条纹仿真

Fig. 3 Simulation of sinusoidal stripe weighted by binary stripes

采集一次,在二进制加权时再对 B_{c5} 和 B_{c6} 重复加权运算一次,仍然可以达到 8 幅二值条纹加权正弦条纹的目的。根据二进制编码方法的特性,通过式(5)~(7)

对 7 种不同采样取值个数进行二进制编码,得到不同重复幅数的多组二值条纹。相同条纹结果具体如表 1 所示。

表 1 采样取值分析

Table 1 Sampling value analysis

Number of gray values	Duplicate stripes	Number of superposition after uniqueness
8	$B_{c2}, B_{c4}, B_{c5}, B_{c7}; B_{c3}, B_{c6}, B_{c8}$	3
9	$B_{c3}, B_{c8}; B_{c4}, B_{c6}, B_{c7}$	5
12	$B_{c3}, B_{c5}, B_{c6}, B_{c7}; B_{c4}, B_{c8}$	4
15	B_{c1}, B_{c6}	7
16	$B_{c5}, B_{c7}; B_{c6}, B_{c8}$	6
18	$B_{c3}, B_{c8}; B_{c6}, B_{c7}$	6
20	B_{c3}, B_{c8}	7

从表 1 可以看出,具有重复条纹的幅数与采样取值个数基本成反比,但采样取值个数的减少也会降低条纹的正弦性。为了减少投影幅数且不损失较多的正弦性,取值个数 M 为 12 时更加符合需求。当取值个数 $M=12$ 时,经过二进制编码过程后,8 幅二值条纹中 B_{c3}, B_{c5}, B_{c6} 和 B_{c7} 重复, B_{c4} 和 B_{c8} 重复,因此在二进制加权时可以对 B_{c3} 复用加权 3 次、 B_{c4} 复用加权一次,以减少 B_{c5}, B_{c6}, B_{c7} 和 B_{c8} 的投影和采集。复用加权运算公式如式(9)所示,编码条纹唯一化原理如图 4 所示。复用加权生成正弦条纹仿真如图 5 所示。

$$I_n^c = \left[\sum_{i=1}^4 (B_{ci}^c - I_b^c) \times 2^{(8-i)} + \sum_{j=3}^1 (B_{cj}^c - I_b^c) \times 2^j + (B_{c4}^c - I_b^c) \right] / 255, n = 1, 2, \dots, N. \quad (9)$$

3 实验与分析

本实验在实验室构建的三维测量系统中进行。该系统主要由 DLP 投影仪 (Light Crafter 4500) 和工业相机 (Point Grey FL3-U3-13Y3M-C) 构成。投影仪的输

入分辨率为 912 pixel × 1140 pixel, 输出分辨率为 1280 pixel × 800 pixel; 工业相机的分辨率为 1280 pixel × 1024 pixel。为了对比二进制编码条纹方法、复用加权方法以及传统方法之间的优劣,进行了多样的对比实验。为了实验对比的客观性和科学性,所涉及方法的条纹周期均设计为 32, 均使用互补格雷码方法进行相位展开。在实验过程中,环境光强、相机焦距、光圈、曝光时间、物体的位姿等外在因素保持一致。

3.1 不同取值实验分析

二进制编码条纹的基本原理是使用编码组成的二值条纹进行二进制加权生成正弦条纹,以此代替直接投影的灰度正弦条纹,实现二值条纹与相移方法的有机结合。在文献[16]中,投影了 3 幅小数部分的二值条纹用于获得更好的正弦性。本实验将二进制编码条纹方法、复用加权方法以及文献[16]方法进行对比分析,不同取值方法的投影分辨率、二值条纹幅数、相移步数、总投影幅数等参数如表 2 所示。

对直径为 50.8140 mm 的标准球进行测量,成像距离约为 35 cm,利用 Geomagic Studio 软件将所得局部点云与拟合标准球进行误差分析,图 6(a)为局部点

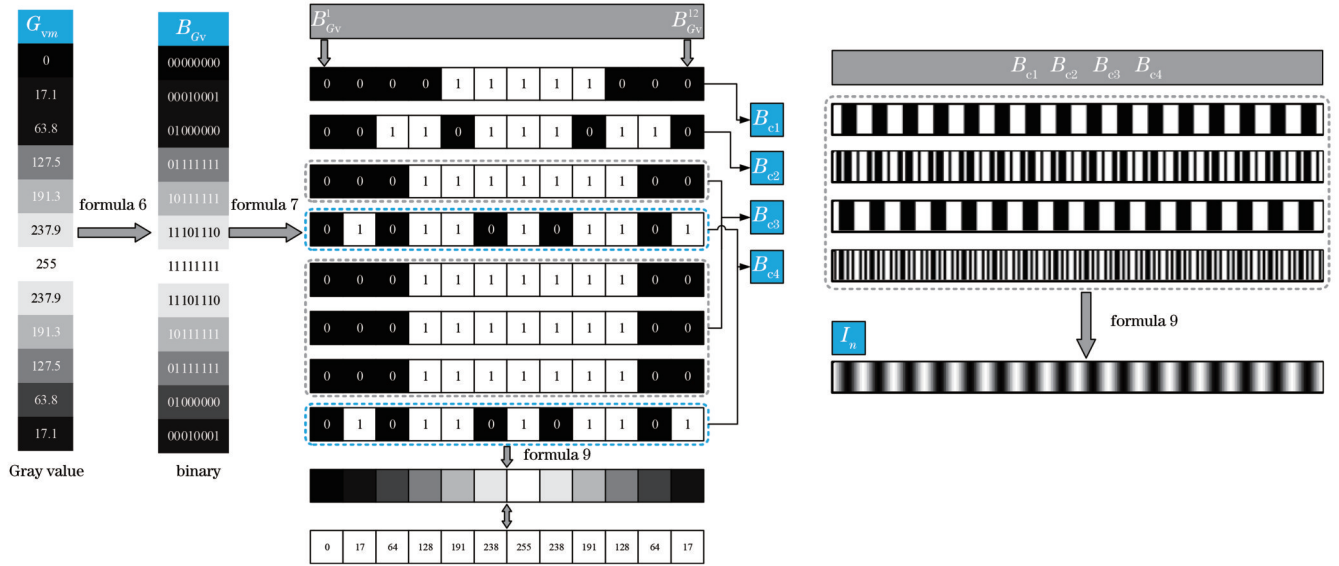


图 4 二进制编码条纹唯一化过程
Fig. 4 The process of the uniqueness of binary coded stripes

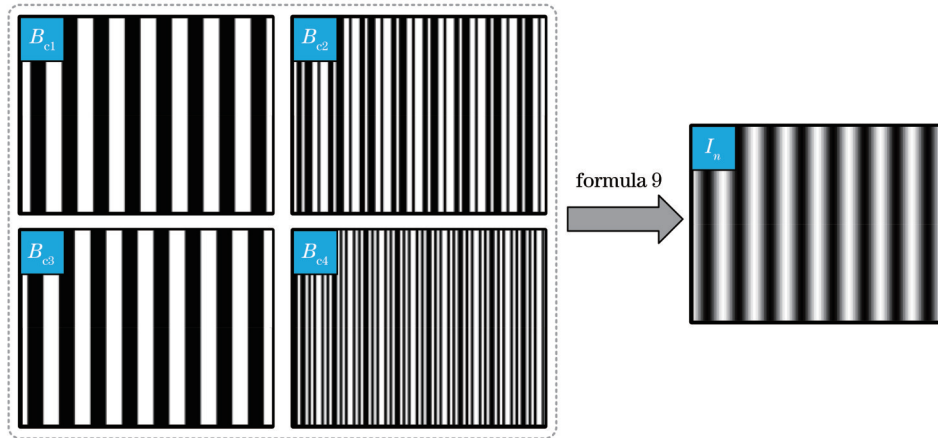


图 5 二值条纹复用加权正弦条纹仿真
Fig. 5 Simulation of reusing weighted sinusoidal stripe by binary stripes

表 2 不同取值投影幅数分析
Table 2 Analysis of projection amplitude of different values

Number of gray values	12	15	18	12	16	20	Literature [16]
Number of superposition	4	7	6	4	6	7	11
Period of stripe	32	32	32	32	32	32	32
Width of stripe /pixel	768	912	912	768	912	912	912
N-step phase-shifting	3	3	3	4	4	4	4
Number of gray codes	6	6	6	6	6	6	6
Number of projections	20	29	26	24	32	36	52

云重建结果,图 6(b)为拟合标准球结果,拟合误差分析结果如表 3 所示。在不同取值方法的对比实验下,局部点云数据与拟合标准球的平均距离相差较小,三步相移优化方法所得平均距离为 0.0153 mm,四步相移优化方法所得平均距离为 0.0107 mm。并对实际物体进行了测量,不同取值方法的重建效果近似,测量结果如图 7 所示。实验结果表明,所提复用加权方法在

降低了 50% 的投影幅数后,仍然可以保持较高的精度和测量效果。

3.2 传统方法对比

为了验证所提方法相比于传统方法的优越性,通过 3 组对照实验与传统三步、四步相移方法进行对比。

1) 为了验证所提方法加权生成条纹的正弦性,对一块高精度棋盘格标定板进行测量,图 8(a)为 4 种方

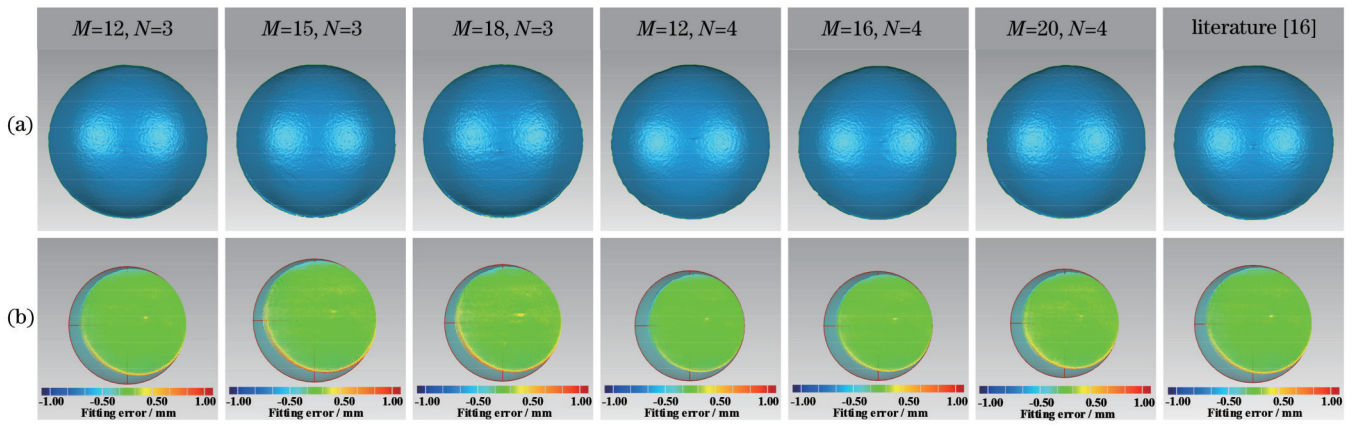


图 6 标准球重建与拟合。(a)局部点云重建结果;(b)拟合误差分布

Fig. 6 Reconstruction and fitting of standard sphere. (a) Results of local point cloud reconstruction; (b) fitting error distribution

表 3 拟合误差分析结果

Table 2 Analysis results of fitting error

Number of values	12	15	18	12	16	20	Literature [16]
N-step phase-shifting	3	3	3	4	4	4	4
Number of point clouds	38326	39562	38977	36072	36715	37103	38411
Average distance /mm	0.0153	0.0381	0.0440	0.0107	0.0160	0.0363	0.0156

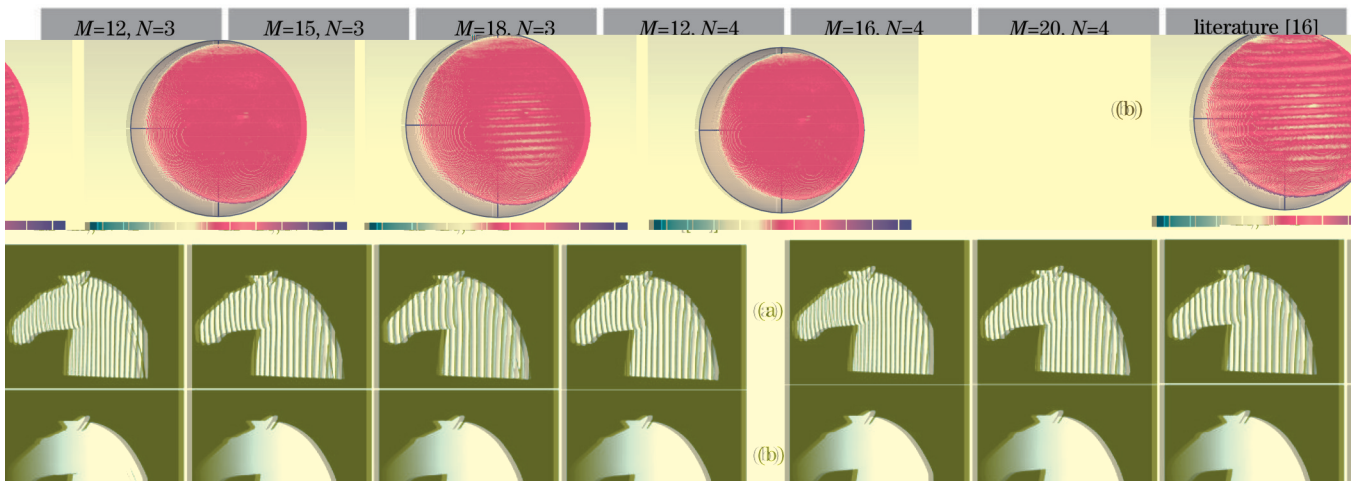


图 7 马头雕塑重建结果。(a)截断相位;(b)绝对相位;(c)局部重建结果

Fig. 7 Reconstruction results of horse head sculpture. (a) Absolute phase; (b) reconstruction results; (c) local reconstruction results

法所得相移条纹图像,其中,第3、4幅为4幅二值条纹复用二进制加权生成。对第820行的451 pixel~750 pixel共300个像素点的灰度值进行正弦拟合,拟合图像如图8(b)所示,条纹正弦拟合误差分析结果如表4所示。由于高精度标定板表面深度近似于线性,同样对第820行的451 pixel~750 pixel共300个像素点的深度值 Z_w 进行直线拟合,拟合图像如图9所示,深度直线拟合误差分析结果如表5所示。实验结果表明:所提方法拟合正弦的均方根误差(RMSE)为3.6082和3.3125,误差平方和(SSE)为3529.3和3028.4,使用复用加权二进制编码条纹方法所获得的正弦条纹的正弦性要优于传统方法;优化方法深度直线拟合的均方根误差为0.0415 mm和0.0388 mm,误

差平方和为0.4804 mm和0.4493 mm,优于传统三步、四步相移方法。

2)为了突出所提方法相比于传统方法的精度优势,进行了精度对比。使用传统三步、四步相移方法对标准球进行测量,并进行局部重建、拟合,与所提优化方法的三步、四步方法进行精度对比,重建结果和拟合图像如图10所示。传统方法所得局部点云与拟合标准球的平均距离为0.0434 mm和0.0561 mm,劣于所提方法的0.0153 mm和0.0107 mm,精度对比结果如表6所示。

3)为了证明所提方法的实际测量效果,分别对表面深度变化较大的石膏头像进行测量,所得重建结果和局部放大如图11所示。从结果来看,传统三步、四

图 8 条纹正弦性拟合对比。(a)相移条纹图像;(b)拟合图像

Fig. 8 Comparison of stripes sinusoidal fitting. (a) Phase shifted fringe images; (b) fitted images

表 4 条纹正弦性拟合误差结果

Table 4 Results of fitting error of sinusoidal stripes

Method	RMSE	SSE
Three-step phase-shifting	5.4732	8267.2
Four-step phase-shifting	5.2263	7538.7
Proposed method/three-step	3.6082	3529.3
Proposed method/four-step	3.3125	3028.4

步相移方法受到系统非线性影响,出现了条状的周期性误差,而所提方法的重建表面效果更佳。

4 结 论

通过对二进制编码条纹方法原理的进一步研究,设计出了更优的采样方案,在进行二进制编码以及二值条纹唯一化处理后,采用复用加权方法生成正弦条纹,以减少实际的二值条纹投影幅数。将 8 幅二值条

表 5 直线拟合误差结果

Table 5 Results of error of line fitting

Method	RMSE /mm	SSE /mm
Three-step phase-shifting	0.0959	2.7378
Four-step phase-shifting	0.0646	1.2451
Proposed method/three-step	0.0415	0.4804
Proposed method/four-step	0.0388	0.4493

图 9 直线拟合图像
Fig. 9 Images of line fitting

图 10 与传统方法的精度对比。(a)局部点云重建结果;(b)拟合误差分布

Fig. 10 Precision comparison with traditional methods. (a) Reconstruction results of local point cloud; (b) fitting error distribution

纹加权生成 1 幅正弦条纹的方法优化为 4 幅,结合三步相移方法和互补格雷码相位展开方法,仅需 20 幅二值条纹即可完成三维测量。多组对比实验结果表明,所提方法在大幅减少二进制编码条纹方法投影幅数的同时,并不会降低测量精度和效果。同时相比于传统相

移方法,所提方法可以大大降低系统的非线性影响,也进一步提升了 DLP 投影仪的投影速率。综上所述,所述方法可以有效减少二进制编码条纹方法的投影幅数,并为基于相移条纹分析的高速三维测量提供了技术思路。

表 6 精度对比结果
Table 6 Comparison results of precision

Method	Number of point clouds	Average distance /mm
Three-step phase-shifting	39916	0.0434
Four-step phase-shifting	39256	0.0561
Proposed method/three-step	38326	0.0153
Proposed method/four-step	36072	0.0107

图 11 大深度物体重建结果。(a)局部点云重建结果(b)局部放大结果

Fig. 11 Reconstruction results of large depth objects. (a) Reconstruction results of local point cloud; (b) results of local amplification

参 考 文 献

- [1] 苏显渝, 张启灿, 陈文静. 结构光三维成像技术[J]. 中国激光, 2014, 41(2): 0209001.
Su X Y, Zhang Q C, Chen W J. Three-dimensional imaging based on structured illumination[J]. Chinese Journal of Lasers, 2014, 41(2): 0209001.
- [2] Song Z, Jiang H L, Lin H B, et al. A high dynamic range structured light means for the 3D measurement of specular surface[J]. Optics and Lasers in Engineering, 2017, 95: 8-16.
- [3] Li Y X, Qian J M, Feng S J, et al. Deep-learning-enabled dual-frequency composite fringe projection profilometry for single-shot absolute 3D shape measurement[J]. Opto-Electronic Advances, 2022, 5(5): 210021.
- [4] Zhang L, Chen Q, Zuo C, et al. Real-time high dynamic range 3D measurement using fringe projection[J]. Optics Express, 2020, 28(17): 24363-24378.
- [5] 陈琦立, 陈文静. 发散圆形条纹投影的共轴三维测量方法[J]. 光学学报, 2022, 42(19): 1912004.
Chen Q L, Chen W J. Coaxial three-dimensional measurement method of divergent circular fringe projection[J]. Acta Optica Sinica, 2022, 42(19): 1912004.
- [6] 王浩然, 吴周杰, 张启灿, 等. 基于时间复用编码的高速三维形貌测量方法[J]. 光学学报, 2023, 43(1): 0112003.
Wang H R, Wu Z J, Zhang Q C, et al. High-speed three-dimensional morphology measurement based on time multiplexing coding[J]. Acta Optica Sinica, 2023, 43(1): 0112003.
- [7] 汪锦航, 卢荣胜, 刘端茂. 高动态范围表面自适应条纹投影测量方法[J]. 光学学报, 2021, 41(19): 1912001.
Wang J H, Lu R S, Liu D M. Adaptive fringe projection measurement method for high dynamic range surface[J]. Acta Optica Sinica, 2021, 41(19): 1912001.
- [8] 陈强华, 周胜, 丁锦红, 等. 基于多步相移法和偏振干涉光学层析光路的三维温度场测量[J]. 光学学报, 2022, 42(7): 0712004.
Chen Q H, Zhou S, Ding J H, et al. Three-dimensional temperature field measurement based on multi-step phase shift method and polarization interference optical tomography optical path[J]. Acta Optica Sinica, 2022, 42(7): 0712004.
- [9] Zhang S. Recent progresses on real-time 3D shape measurement using digital fringe projection techniques[J]. Optics and Lasers in Engineering, 2010, 48(2): 149-158.
- [10] Zuo C, Feng S J, Huang L, et al. Phase shifting algorithms for fringe projection profilometry: a review[J]. Optics and Lasers in Engineering, 2018, 109: 23-59.
- [11] 郭志明, 张启灿, 麻珂. 三维形测量中结构光场的非线性分析和校正[J]. 激光杂志, 2011, 32(1): 14-16.
Guo Z M, Zhang Q C, Ma K. Analysis and correction of the nonlinearity of the structured light illumination in three-dimensional shape measurement[J]. Laser Journal, 2011, 32(1): 14-16.
- [12] Zhang S, Yau S T. Generic nonsinusoidal phase error correction for three-dimensional shape measurement using a digital video projector[J]. Applied Optics, 2007, 46(1): 36-43.
- [13] 郑东亮, 达飞鹏. 双步相移光栅投影测量轮廓术[J]. 光学学报, 2012, 32(5): 0512004.
Zheng D L, Da F P. Double-step phase-shifting algorithm for fringe projection measurement[J]. Acta Optica Sinica, 2012, 32(5): 0512004.
- [14] Su X Y, Zhou W S, von Bally G, et al. Automated phase-measuring profilometry using defocused projection of a Ronchi grating[J]. Optics Communications, 1992, 94(6): 561-573.
- [15] 严飞, 祁健, 刘银萍, 等. 一种二值编码条纹聚焦投影的三维测量方法[J]. 光学学报, 2022, 42(22): 2212002.
Yan F, Qi J, Liu Y P, et al. Three-dimensional measurement method for binary-coded fringe focus projection[J]. Acta Optica

- Sinica, 2022, 42(22): 2212002.
- [16] 刘佳, 路长秋, 文杰, 等. 基于二进制编码条纹的三维测量方法[J]. 光学学报, 2023, 43(1): 0112004.
Liu J, Lu C Q, Wen J, et al. Three-dimensional measurement method based on binary coded fringes[J]. Acta Optica Sinica, 2023, 43(1): 0112004.
- [17] 张启灿, 吴周杰. 基于格雷码图案投影的结构光三维成像技术[J]. 红外与激光工程, 2020, 49(3): 0303004.
Zhang Q C, Wu Z J. Three-dimensional imaging technique based on Gray-coded structured illumination[J]. Infrared and Laser Engineering, 2020, 49(3): 0303004.
- [18] Hu P Y, Yang S M, Zheng F H, et al. Accurate and dynamic 3D shape measurement with digital image correlation-assisted phase shifting[J]. Measurement Science and Technology, 2021, 32(7): 075204.
- [19] 李中伟. 基于数字光栅投影的结构光三维测量技术与系统研究[D]. 武汉: 华中科技大学, 2009.
Li Z W. Research on structured light 3D measuring technology and system based on digital fringe projection[D]. Wuhan: Huazhong University of Science and Technology, 2009.
- [20] 孙学真, 苏显渝, 邹小平. 基于互补型光栅编码的相位展开[J]. 光学学报, 2008, 28(10): 1947-1951.
Sun X Z, Su X Y, Zou X P. Phase-unwrapping based on complementary structured light binary code[J]. Acta Optica Sinica, 2008, 28(10): 1947-1951.

Three-Dimensional Measurement Method of Reusing Weighted Binary Coded Stripes

Yan Fei^{1,2}, Lu Changqiu¹, Wen Jie¹, Xiao Yuqian¹, Liu Jia^{1,2*}

¹College of Automation, Nanjing University of Information Science and Technology, Nanjing 210044, Jiangsu, China;

²Collaborative Innovation Center of Atmospheric Environment and Equipment Technology, Nanjing 210044, Jiangsu, China

Abstract

Objective There are two primary three-dimensional (3D) measurement error sources of structural light based on the phase shift method: phase shift error and nonlinear error. With the development of a digital projector, the computer can produce standard sinusoidal stripes to eliminate the phase shift error. However, the nonlinear error of the projector and camera will cause the stripe to lose particular sinusoidal properties, affecting the measurement accuracy and effect. To reduce the nonlinear error of the system, global scholars have put forward various solutions, among which the binary stripe method is the most widely studied. The binary stripe is not affected by nonlinearity because it has only two gray values. The projection speed can be significantly improved by a digital projector projecting 1-bit binary stripes. In the study of many binary stripes, the binary coded stripe method uses multiple binary stripes to generate a sinusoidal stripe, which avoids defocusing projection, effectively reduces the nonlinear effect of the system, and improves measurement accuracy and projection efficiency. Based on the binary coded stripe method, this paper proposes a method of reusing weighted binary coded stripes, which significantly reduces the number of binary stripes weighted with a sinusoidal stripe and further improves the projection efficiency.

Methods This paper proposes a method of reusing weighted binary coded stripes. The binary coded stripe method samples the gray value of sinusoidal stripes uniformly to obtain the discrete decimal gray values of a sinusoidal stripe. The gray values are then processed by binary coding, and all of the code words with the same level of binary code words are combined to generate binary stripes. After sequential projection by a digital projector, the collected stripe images are weighted in binary to generate a sinusoidal stripe modulated by object depth information. In the implementation process of binary coded stripes, a certain number of repeated binary stripes will appear under a specific gray-value sampling number. After comparison, 12 gray values are uniformly sampled within a sinusoidal period, and the binary coding generates binary stripes. After unique processing, the same binary stripes only need to be projected once, and repeated weighting is performed in the calculation process. As a result, only four binary stripes are required to generate a sinusoidal stripe. Finally, the method is combined with the three-step phase shift technique. The complementary gray code method is also used to carry out the phase unwrapping, which can realize an efficient 3D measurement with 20 binary stripes in the state of constant focus.

Results and Discussions This paper uses the proposed method, three-step phase shift method, and the four-step phase shift method to measure different objects and carry out comparison experiments of different gray values, and the comparison experiment with the traditional methods aims to verify the superiority of the method of reusing weighted binary

coded stripes. In the first experiment, through the measurement of a standard sphere, the average distance difference between local point cloud data obtained by different gray values and fitted standard sphere is small. The average distance obtained by the three-step phase shift optimization method is 0.0153 mm, and that by the four-step phase shift optimization method is 0.0107 mm (Fig. 6 and Table 3). As shown in Fig. 7, the actual item is measured, and the reconstructed results are comparable, which verifies that the proposed method of reusing weighted binary coded stripes can still maintain high accuracy and measurement impact after reducing the number of projections. In the comparison experiment with the traditional methods, sinusoidal fitting is carried out on the sinusoidal stripe obtained by the traditional methods and the proposed method. The root-mean-square error (RMSE) of the sinusoidal fitting is 3.6082 and 3.3125, and the sum of squared errors (SSE) is 3529.3 and 3028.4 (Fig. 8 and Table 4). Linear fitting is performed on the measurement results of the high-precision plane. The RMSE is 0.0415 and 0.0388 mm, respectively, and the SSE is 0.4804 and 0.4493 mm (Fig. 9 and Table 5). As demonstrated in Fig. 10 and Table 6, after measuring the standard sphere, the average distance between the local point cloud and the fitted standard sphere is reduced by 72.3% when compared with that by the traditional three-step phase shift method. For the measurement of the plaster head, whose surface depth varies greatly, the traditional three-step and four-step phase shift methods have strip-like systematic errors due to the nonlinear effects of the system. However, the surface reconstruction effect of the proposed method is better (Fig. 11).

Conclusions This paper proposes a method of reusing weighted binary coded stripes. A better sampling scheme is designed by further studying the principle of the binary coded stripe method. After the unique processing of binary coding and binary stripes, the method of reusing weighted binary coded stripes generates sinusoidal stripes to reduce the actual projection number of binary stripes. In order to generate a sinusoidal stripe, eight weighted binary stripes are reduced to four binary stripes. As a result, only 20 binary stripes are required to complete the 3D measurement by the three-step phase shift method and the complementary gray code phase unwrapping method. The results of comparison experiments show that the proposed method will not reduce the measurement accuracy and effect while significantly reducing the projection number by the binary coded stripe method. Compared with the traditional phase shift method, the proposed method can significantly reduce the nonlinear effect of the system and further improve the projection rate of the DLP projector. In conclusion, the proposed method effectively reduces the projection number required by the binary coded stripe method and provides technical support for high-speed 3D measurement based on phase shift stripe analysis.

Key words three-dimensional measurement; phase shift technology; binary coding; binary stripe; nonlinear